24th COBEM - 2017

24th ABCM International Congress of Mechanical Engineering
December 3-8, 2017, Curitiba, PR, Brazil

COBEM-2017-1453
LQR CONROL FOR A SELF-BALACING UNICYCLE

Gabriel Pereira das Neves[1]
Bruno Augusto Angélico[2]
[1,2]Dept. of Telecommunications and Control Engineering, Escola Politécnica da Universidade de São Paulo, São Paulo - Brazil
[1] gabriel.pereira.neves@usp.br, [2]angelico@usp.br.

Abstract. *This work presents a unicycle with reaction wheel, showing the modeling, the design and testing of the stabilizing controller. A three-dimensional drawing was generated (3D CAD) to assist the construction. The prototype was constructed by attaching the electronic components, the battery, the wheels and the motors to a body, to make it fully autonomous. The positioning of the parts has to be balanced, trying to maintain the position of the center of mass along the vertical and horizontal axis of symmetry. Then the system was modeled by the Lagrange method, and a linear quadratic regulator (LQR) was designed to stabilize the plant. This paper presents the simulation of the LQR controller, which has shown good results.*

Keywords: *Unicycle, LQR, Optimal control, Bryson's rule, System modeling*

1. INTRODUCTION

For robotic systems, the issue of balance is of fundamental importance. Several control studies approach this theme, and the most classic and didactic is the case of the inverted pendulum.

Many variations of the classical pendulum emerged over time, such as the Furuta pendulum (Furuta *et al.* (1991)) and the pendulum with reaction wheel (Jepsen *et al.* (2009)), which uses the torque reaction applied in a wheel to stabilize it. This concept was expanded to the 3-D inverted pendulum, in the form of a cube, with reaction wheel (Muehlebach and D'Andrea (2017)).

The use of reaction wheel as actuator is widely used for space systems and satellites (Chou *et al.* (2011)), as well as in other control systems, such as the pendulums already mentioned, stabilization and assistance for motorcycle (Tanos *et al.* (2014)) and bipedal robot systems (Brown and Schmiedeler (2016)).

Another widely used variation today is the segway (Bin *et al.* (2010)), that is a locomotion system with two wheels, which is based on the inverted pendulum.

In this work there is a variation of an equilibrium system very similar to a segway but with only one wheel in contact with the ground, and using a reaction wheel to stabilize the roll angle.

Other works about self-balancing unicycle with one reaction wheel can be found in (Han and Lee (2015)), (Lee *et al.* (2013)).

2. CONSTRUCTION

The unicycle is separate in three parts, the body, the reaction wheel and the travel wheel in contact with the ground, as shows Figure 1.

The prototype was built to be totally autonomous, so, all components were attached on the body and the power is supplied by a battery, as can be seen in Figure 2(b).

The reaction wheel, which is responsible for the roll angle control, was fixed on the highest part and the travel wheel responsible for the pitch angle control, on the lower part. Figure 2 shows the built prototype.

An important point about the system construction is the fact that the travel wheel has a convex curved pattern ensuring a point contact to the ground.

Both wheels are actuated by DC motors with reduction gearbox, but, this system required high operation torque, which can cause damage to the gears. So, a first order filter was considered to protect the gearboxes.

The dynamic torque can be approximated by

$$\tau_d \approx \frac{|\Delta\omega|}{\Delta t} J, \tag{1}$$

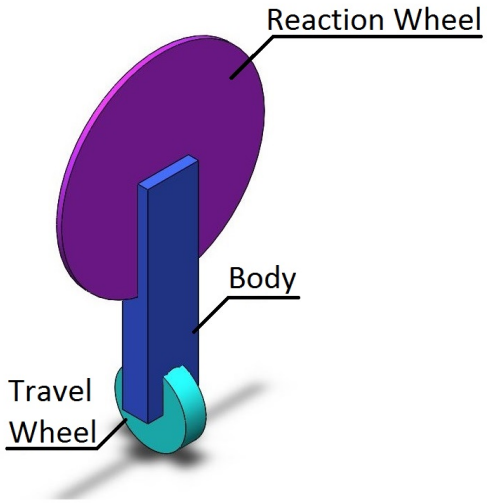

Figure 1. Schematic drawing.

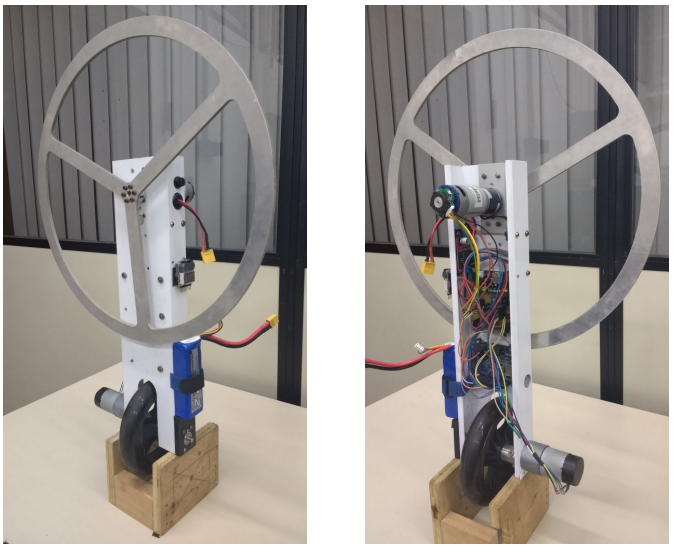

(a) View 1. (b) View 2.

Figure 2. Practical unicycle

where $\Delta\omega$ is the angular velocity variation, J is the moment of inertia and Δt is the time variation. In the worst case

$$\tau_d \approx \frac{2\omega}{\Delta t} J, \tag{2}$$

where ω is the maximum speed of the motor after de gear box. Thus, if the controller change the rotation direction very fast ($\Delta t \to 0$) the dynamic toque tends to ∞. In order to protect the gearbox, a first order filter is considered

$$G_{lpf} = \frac{30}{s + 30}, \tag{3}$$

where s is the variable of the Laplace transformation. The time constant of this filter is $\tau_t = 1/30\ [s]$. Therefore, for a step response, the system will take $4\tau_t$, which is equal to 0.133 second, to reach 98% of the maximum value.

Considering the worst case for the reaction wheel motor (maximum speed of 118 rpm), the dynamic torque is

$$\tau_d = \frac{2(118 \times 2 \times \pi/60)}{0.1333} \times 0.013472 = 2.4971[Nm], \tag{4}$$

which is lower than half the stall torque of the motor (approximately $6\ [Nm]$), thus, the gearbox is protected from overload by the dynamic torque.

The parameter of the prototype is shown in Table 1.

Table 1. Physical Parameters

	Parameter	Value
R_r	Reaction wheel radius $[m]$	0.2
R_w	Wheel radius $[m]$	0.071
L	Distance of the center of mass (CM) of the body $[m]$	0.18632
d	Distance between the CM of the body and reaction wheel $[m]$	0.1503
M_r	Reaction wheel mass $[Kg]$	0.47568
M_b	Body mass $[Kg]$	1.23913
M_w	Wheel mass $[Kg]$	0.30220
g	Acceleration of gravity $[m/s^2]$	9.8
J_r	Reaction wheel moment of inertia $[Kgm^2]$	0.013472
J_w	Wheel moment of inertia $[Kgm^2]$	0.00077
J_{br}	Moment of inertia of the body plus reaction wheel $[Kgm^2]$	0.03937
J_{bw}	Moment of inertia of the body plus wheel $[Kgm^2]$	0.03458
n_r	Reduction of the reaction wheel motor	71
K_{tr}	Torque constant of the reaction wheel motor $[Nm/A]$	0.3383
K_{er}	Electrical constant of the reaction wheel motor $[Vs^2/rad]$	0.9454
R_{er}	Electrical resistance of the reaction wheel motor$[\Omega]$	0.6
n_w	Reduction of the wheel motor	131.25
K_{tw}	Torque constant of the wheel motor $[Nm/A]$	0.3531
K_{ew}	Electrical constant of the reaction wheel motor $[Vs^2/rad]$	1.3465
R_{ew}	Electrical resistance of the wheel motor$[\Omega]$	2.4
B_{vw}	Travel wheel viscous friction $[Ns^2/rad]$	0.1
B_{vr}	Reaction wheel viscous friction $[Ns^2/rad]$	0.1

3. SYSTEM MODELING

The unicycle has three parts, theirs center of mass are determined by $\overrightarrow{p_1}$, $\overrightarrow{p_2}$ and $\overrightarrow{p_3}$, respectively, for the position of the travel wheel, body and reaction wheel (Han and Lee (2015)), as is shown in Figure 3.

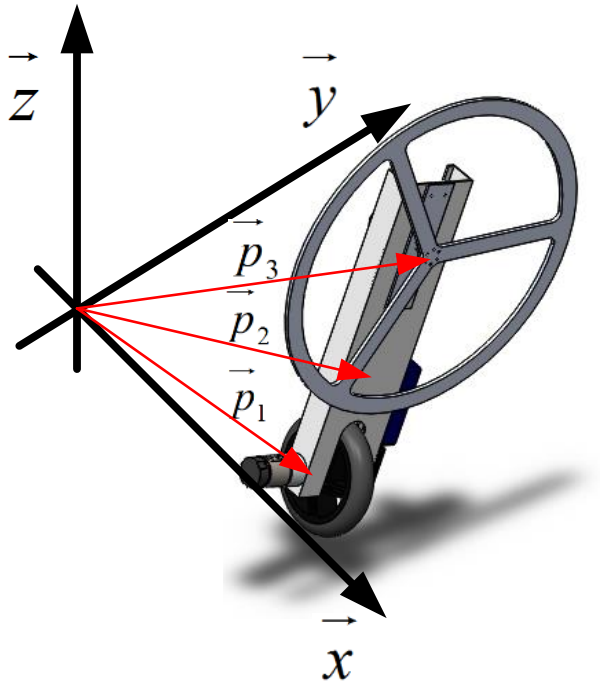

Figure 3. Bodies position.

$$\overrightarrow{p_1} = \begin{bmatrix} R_w\theta_w & R_w\sin(\varphi) & R_w\cos(\varphi) \end{bmatrix}, \tag{5}$$

$$\overrightarrow{p_2} = \begin{bmatrix} R_w\theta_w + L\sin(\psi) & (R_w + L\cos(\psi))\sin(\varphi) & (R_w + L\cos(\psi))\cos(\varphi) \end{bmatrix}, \tag{6}$$

$$\overrightarrow{p_3} = \begin{bmatrix} R_w\theta_w + (L+d)\sin(\psi) & (R_w + (L+d)\cos(\psi))\sin(\varphi) & (R_w + (L+d)\cos(\psi))\cos(\varphi) \end{bmatrix}. \tag{7}$$

3.1 Energy Calculation

The translational kinetic energy is calculated by

$$E_T = \frac{1}{2}\overrightarrow{v}^\top M \overrightarrow{v}, \tag{8}$$

where M is the mass of the object and $\overrightarrow{v}$ is the velocity vector of the center of mass in relation to the inertial system. Thus, the translational kinetic energy of the unicycle is given by

$$E_T = \frac{1}{2}\overrightarrow{v_1}^\top M_w \overrightarrow{v_1} + \frac{1}{2}\overrightarrow{v_2}^\top M_b \overrightarrow{v_2} + \frac{1}{2}\overrightarrow{v_3}^\top M_r \overrightarrow{v_3}, \tag{9}$$

where,

$$\overrightarrow{v_1} = \frac{d}{dt}\overrightarrow{p_1}, \tag{10}$$

$$\overrightarrow{v_2} = \frac{d}{dt}\overrightarrow{p_2}, \tag{11}$$

$$\overrightarrow{v_3} = \frac{d}{dt}\overrightarrow{p_3}. \tag{12}$$

The rotational kinetic energy is calculated as

$$E_R = \underbrace{\frac{1}{2}J_w\dot{\theta}_w^2}_{1} + \underbrace{\frac{1}{2}J_{br}\dot{\psi}^2}_{2} + \underbrace{\frac{1}{2}J_r(\dot{\theta}_r + \dot{\varphi})^2}_{3} + \underbrace{\frac{1}{2}J_{bw}\dot{\varphi}^2}_{4}, \tag{13}$$

where, part 1 corresponds to the travel wheel rotation, part 2 is the rotation of the pitch angle, part 3 corresponds to the rotation of the reaction wheel and its center of mass, part 4 is the rotation of the roll angle.

The potential energy of a body with mass M and height of its center of mass in relation to a reference plane given by h is calculated as

$$U = Mgh. \tag{14}$$

In this problem, the ground is considered to be the reference plane, the height is the projection of vectors $\overrightarrow{p_1}$, $\overrightarrow{p_2}$ and $\overrightarrow{p_3}$ on the $\overrightarrow{z}$ axis, hence, the potential energy of the unicycle is calculated as

$$U = M_w g R_w \cos(\varphi) + M_b g((R_w + L\cos(\psi))\cos(\varphi)) + M_r g(R_w + (L+d)\cos(\psi))\cos(\varphi). \tag{15}$$

3.2 Lagrange Equation

The Lagrange equation is used to determine the dynamic model of the system Craig (2005). The Lagrangian is defined as

$$L = E_T + E_R - U. \tag{16}$$

Given $q = \begin{bmatrix}\theta_r & \varphi & \theta_w & \psi\end{bmatrix}^\top$ (vector of the variables corresponding to the degrees of freedom), and τ the vector of external torques and force, the Lagrange equation is written as

$$\frac{d}{dt}\frac{\partial L}{\partial \dot{q}} - \frac{\partial L}{\partial q} = \tau - B_v, \tag{17}$$

where $B_v = \begin{bmatrix}B_{vr}\theta_r & -B_{vr}\theta_r & B_{vw}\theta_w & -B_{vw}\theta_w\end{bmatrix}^\top$ is the vector of the viscous friction, where B_{vr} and B_{vw} the viscous friction coefficients of the reaction and travel wheel, respectively.

In this case, the external torque is caused by the motors and their reactions, such that

$$\tau = \begin{bmatrix}\tau_r & -\tau_r & \tau_w & -\tau_w\end{bmatrix}^\top, \tag{18}$$

where, τ_r is the torque caused by the motor connected to the reaction wheel, and τ_w the torque caused by the motor connected to the travel wheel. The equations of the DC motors are

$$\tau_r = \frac{n_r K_{tr}}{R_{er}}(12PWM_r - K_{er} n_r \dot{\theta_r}), \tag{19}$$

$$\tau_w = \frac{n_w K_{tw}}{R_{ew}}(12PWM_w - K_{ew}(n_w \dot{\theta_w} - \dot{\psi})), \tag{20}$$

where, PWM_r and PWM_w are the PWM duty cycle of the motor coupled with the reaction wheel and the travel wheel, respectively.

The linear model presents the characteristics of the system around the operation point. The first point that can be observe is the uncoupled characteristic

$$A = \begin{bmatrix}A_r & 0\\ 0 & A_w\end{bmatrix}, \tag{21}$$

$$B = \begin{bmatrix}B_r & 0\\ 0 & B_w\end{bmatrix}, \tag{22}$$

which results in

$$G = \begin{bmatrix}G_r & 0\\ 0 & G_w\end{bmatrix}, \tag{23}$$

where, G is the transfer matrix.

As verified, the pitch and roll angle are uncoupled, in other words, $\begin{bmatrix}\varphi & \dot{\varphi} & \dot{\theta_r} & \tau_r\end{bmatrix}$ does not interfere in $\begin{bmatrix}\psi & \dot{\psi} & \dot{\theta_w} & \tau_w\end{bmatrix}$ and vice versa.

The linear system was discretized considering zero order hold and a sample time $Ts = 0.01s$. This discrete time linear system is given by:

$$\Phi = \begin{bmatrix} 1.0000 & 0.0070 & -0.0009 & -0.0000 & 0 & 0 & 0 & 0 \\ 0 & 0.4639 & -0.1533 & -0.0009 & 0 & 0 & 0 & 0 \\ 0 & 0.0003 & 1.0011 & 0.0100 & 0 & 0 & 0 & 0 \\ 0 & 0.0527 & 0.2132 & 1.0011 & 0 & 0 & 0 & 0 \\ 0 & 0 & 0 & 0 & 1.0000 & 0.0074 & -0.0058 & 0.0017 \\ 0 & 0 & 0 & 0 & 0 & 0.5305 & -1.0150 & 0.3062 \\ 0 & 0 & 0 & 0 & 0 & 0.0006 & 1.0025 & 0.0096 \\ 0 & 0 & 0 & 0 & 0 & 0.1090 & 0.4669 & 0.9301 \end{bmatrix}, \tag{24}$$

$$\Gamma = \begin{bmatrix} 0.0219 & 0 \\ 3.8878 & 0 \\ -0.0022 & 0 \\ -0.3823 & 0 \\ 0 & 0.0157 \\ 0 & 2.7907 \\ 0 & -0.0036 \\ 0 & -0.6453 \end{bmatrix}. \tag{25}$$

4. LQR CONTROL

The linear quadratic regulator (LQR) is a linear control which it is designed to minimize a certain cost function (Franklin *et al.* (2006))

$$J = \sum_{k=0}^{\infty} x[k]^\top Q x[k] + u[k]^\top R u[k], \tag{26}$$

where, Q and R are semi-definite positive matrices of weighting. The solution of this problem is a state feedback as

$$u[k] = -Kx[k]. \tag{27}$$

A first choice for matrices Q and R is given by Bryson's rule Franklin *et al.* (2006). This technique is a form of normalization of the state variables, so, it is strongly recommend to system with state variables with different units with this rule, Q and R are diagonal matrix such that,

$$Q_{ii} = \frac{1}{\textit{maximum variation accepted of } x_i^2}, \tag{28}$$

and,

$$R_{jj} = \frac{1}{\textit{maximum variation accepted of } u_j^2}, \tag{29}$$

where, ii and jj are the line and column of the matrices Q and R, respectively.

Although Bryson's rules is a practical form to determine matrices Q and R, oftentimes it is not enough, but it is a good starting point to a trial-and-error procedure.

Considering

$$Q = \begin{bmatrix} 0.0065 & 0 & 0 & 0 & 0 & 0 \\ 0 & 14.5903 & 0 & 0 & 0 & 0 \\ 0 & 0 & 0.01 & 0 & 0 & 0 \\ 0 & 0 & 0 & 0.0065 & 0 & 0 \\ 0 & 0 & 0 & 0 & 14.5903 & 0 \\ 0 & 0 & 0 & 0 & 0 & 0.01 \end{bmatrix}, \tag{30}$$

and

$$R = \begin{bmatrix} 1 & 0 \\ 0 & 1 \end{bmatrix}, \tag{31}$$

the control gain resulted in

$$K_{LQR} = \begin{bmatrix} -0.2819 & -14.5076 & -3.1595 & 0 & 0 & 0 \\ 0 & 0 & 0 & -0.3410 & -9.3838 & -1.6206 \end{bmatrix}. \tag{32}$$

5. RESULTS

Two tests were considered, being the first a simulation of the LQR control without considering disturbances such as measurement noise and dead zone of the actuators. Figure 4 shows this simulation. Initial condition of $-5°$ of φ and $5°$ of ψ are considered.

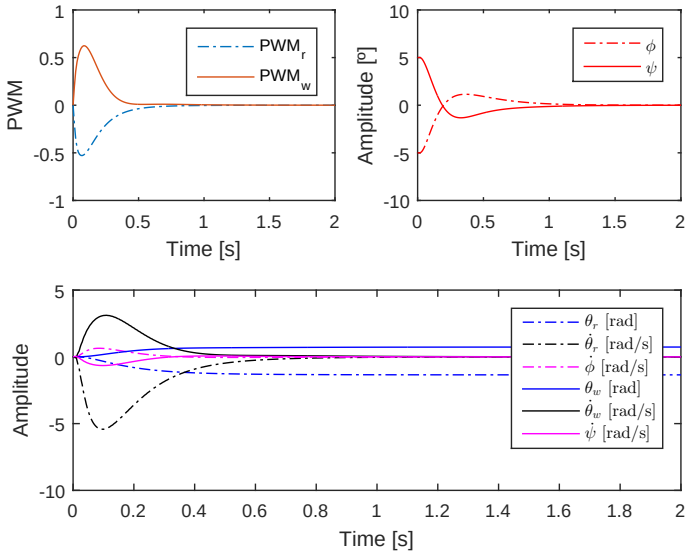

Figure 4. Simulation of the discrete LQR.

As verified, the controller can stabilize the plant without saturating the actuators. Variables θ_r and θ_w (which are respectively the angular position of the reaction wheel and the travel wheel) stabilize at non-zero points, which was expected because these states were removed for the controller project.

Figure 5 shows the torque applied to each motor. As observed, the torque remained much smaller that the stall toque of 6 [Nm].

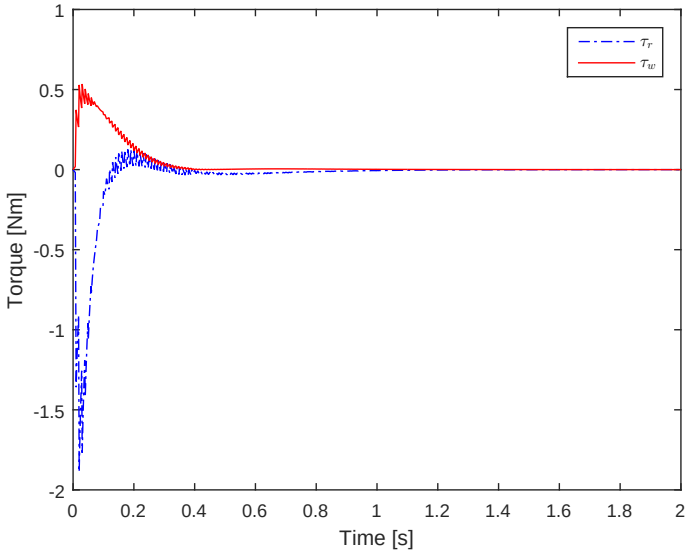

Figure 5. Control effort of the discrete LQR.

Figure 6 shows the simulation results of the controller considering measurement noise (a white noise with variance $10^{-4}[rad]$ and $10^{-4}[rad/s]$) and dead zone of the actuators (12% to the lower wheel and 9% to the reaction wheel). As verified, even with the noise and the dead zone, the controller stabilized the plant.

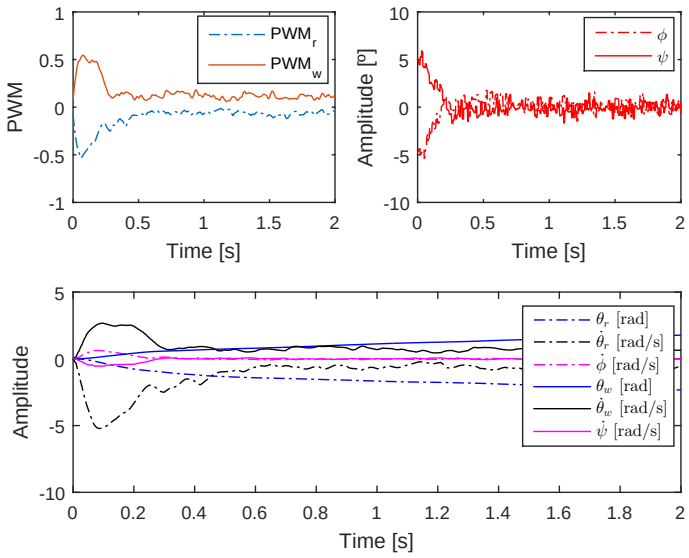

Figure 6. Simulation of the discrete LQR considered noise and dead zone.

6. CONCLUSION

This work shows the concept of a unicycle with reaction wheel, the construction and the stabilizing control.

The first order filter applied to the control signal protected the gearbox against the high dynamic torque caused by the rapid vartiation of the reaction wheel velocity.

The simulation of the controllers presented good results, and the main objective, the stabilization of the unicycle, was achieved.

7. ACKNOWLEDGEMENTS

The authors would like to thank Fundação de Amparo à Pesquisa do Estado de São Paulo (FAPESP) for the grant 2016/00729-9.

8. REFERENCES

Bin, H., Zhen, L.W. and Feng, L.H., 2010. "The kinematics model of a two-wheeled self-balancing autonomous mobile robot and its simulation". In *Conference...* Computer Engineering and Applications (ICCEA), Vol. 2, pp. 64–68.

Brown, T.L. and Schmiedeler, J.P., 2016. "Reaction wheel actuation for improving planar biped walking efficiency". *IEEE Transactions on Robotics*, Vol. 32, No. 5, pp. 1290–1297. ISSN 1552-3098. doi:10.1109/TRO.2016.2593484.

Chou, M.C., Liaw, C.M., Chien, S.B., Shieh, F.H., Tsai, J.R. and Chang, H.C., 2011. "Robust current and torque controls for pmsm driven satellite reaction wheel". *IEEE Transactions on Aerospace and Electronic Systems*, Vol. 47, No. 1, pp. 58–74. ISSN 0018-9251. doi:10.1109/TAES.2011.5705659.

Craig, J.J., 2005. *Introduction to Robotic: Mechanics and Control*. Personal Education International, 3rd edition. ISBN 0-13-123629-6.

Franklin, G., Powell, J. and Workman, M., 2006. *Digital Control of Dynamic Systems*. Ellis-Kagle Press, 3rd edition.

Furuta, K., Yamakita, M. and Kobayashi, S., 1991. "Swing up control of inverted pendulum". In *Conference...* Industrial Electronics, Control and Instrumentation, pp. 2193–2198 vol.3. doi:10.1109/IECON.1991.239008.

Han, S.I. and Lee, J.M., 2015. "Balancing and velocity control of a unicycle robot based on the dynamic model". *IEEE Transactions on Industrial Electronics*, Vol. 62, No. 1, pp. 405–413.

Jepsen, F., Soborg, A., Pedersen, A.R. and Yang, Z., 2009. "Development and control of an inverted pendulum driven by a reaction wheel". In *Conference...* International Conference on Mechatronics and Automation, pp. 2829–2834. ISSN 2152-7431. doi:10.1109/ICMA.2009.5246460.

Lee, J., Han, S. and Lee, J., 2013. "Decoupled dynamic control for pitch and roll axes of the unicycle robot". *IEEE Transactions on Industrial Electronics*, Vol. 60, No. 9, pp. 3814–3822.

Muehlebach, M. and D'Andrea, R., 2017. "Nonlinear analysis and control of a reaction-wheel-based 3-d inverted pendulum". *IEEE Transactions on Control Systems Technology*, Vol. 25, No. 1, pp. 235–246. ISSN 1063-6536. doi: 10.1109/TCST.2016.2549266.

Tanos, A., Steffen, T. and Mavros, G., 2014. "Improving lateral stability of a motorcycle via assistive control of a reaction wheel". In *Conference...* UKACC International Conference on Control, pp. 80–85. doi: 10.1109/CONTROL.2014.6915119.

9. RESPONSIBILITY NOTICE

The following text, properly adapted to the number of authors, must be included in the last section of the paper: The author(s) is (are) the only responsible for the printed material included in this paper.